

## ROSAT OBSERVATIONS OF THE SOMBRERO GALAXY: DISCOVERY OF AN X-RAY ACTIVE NUCLEUS

G. FABBIANO AND J. Z. JUDA

Harvard-Smithsonian Center for Astrophysics, 60 Garden Street, Cambridge, MA 02138

Received 1996 April 10; accepted 1996 September 4

### ABSTRACT

The analysis of a high-resolution X-ray image of NGC 4594, obtained with the *ROSAT* HRI, shows at least three components of the X-ray emission. The most striking one is a pointlike source associated with the LINER nucleus, with (0.1–2.4) keV  $L_x \sim 3.5 \times 10^{40}$  ergs s<sup>-1</sup>. Comparison of the X-ray, H $\alpha$ , and radio emission of this source with those of active galactic nuclei suggests that it may be a low-luminosity version of the latter. If the X-ray emission is due to accretion onto the  $5 \times 10^8 M_\odot$  black hole that may be present at the nucleus of NGC 4594, the accretion rates must be very low, since the luminosity is extremely sub-Eddington. Alternatively, the source may be heavily obscured and only reprocessed photons are detected in the *ROSAT* range. We also detect clumpy emission associated with the disk of NGC 4594, and diffuse (or not resolved) emission from the bulge. With the present data, including a reanalysis of the archival *ROSAT* PSPC observation of this galaxy, we cannot determine how much of this diffuse emission is due to a hot interstellar medium, and how much is instead due to the integrated emission of a population of evolved stellar sources.

*Subject headings:* black hole physics — galaxies: active — galaxies: individual (M104) — galaxies: nuclei — X-rays: galaxies

### 1. INTRODUCTION

NGC 4594, also known as M104, and nicknamed the Sombrero galaxy, is an edge-on luminous Sa. This galaxy has been recently the center of noticeable interest, because it may host a massive  $\sim 5 \times 10^8 M_\odot$  black hole at its nucleus (Kormendy 1988; see Kormendy & Richstone 1995). The nucleus has also been identified as a LINER (Heckman 1980) and hosts a compact and variable radio continuum source (e.g., Hummel, van der Hulst, & Dickey 1984; Bajaja et al. 1988). It shows up as a pointlike source in a *HST* high-resolution image (Crane et al. 1993).

In X-rays, NGC 4594 has been previously observed with low angular resolution ( $\sim 50''$ ) with the *Einstein Observatory* IPC (Giacconi et al. 1979). Its X-ray luminosity was included in a list of LINERs by Halpern & Steiner (1983). However, subsequent, more detailed work showed an extended source centered on the galaxy nucleus (see Forman, Jones, & Tucker 1985; Fabbiano, Kim, & Trinchieri 1992). Although morphologically its prominent bulge may suggest that NGC 4594 may have X-ray properties similar to those of E and S0 galaxies, and in particular be dominated by a hot gaseous halo (Forman et al. 1985), its *Einstein* X-ray spectral parameters and X-ray colors are consistent with those of spiral galaxies and slightly harder than those of E and S0 (Kim, Fabbiano, & Trinchieri 1992a, 1992b). These spectral properties would suggest a predominance of harder X-ray sources in NGC 4594, similar to the population of binary X-ray sources present in spiral galaxies (see Fabbiano 1989). Its X-ray to optical ratio is consistent with those of spiral galaxies, or low-luminosity E and S0, again suggesting that the emission may not be dominated by a hot gaseous halo. This in itself, however, does not exclude the presence of some hot interstellar medium (ISM) at a low level (e.g., Pellegrini & Fabbiano 1994; Fabbiano & Schweizer 1995), and more direct evidence is needed. Some gaseous, possibly extended emission is suggested by the *ASCA* data of this galaxy (Terashima et al. 1994). Moreover, a nuclear source, if present, may have

been responsible for the relatively hard *Einstein* spectrum. Such a source is suggested by the *ASCA* spectrum (Terashima et al. 1994; Serlemitsos, Ptak, & Yaqoob, 1996).

Understanding the composition of the X-ray emission and in particular the role played by the hot ISM is important, if we want to use X-ray observations of a galaxy to measure its binding mass (see Fabbiano 1989). For NGC 4594, in particular, the validity of the *Einstein* mass determination, based on the assumption that the X-ray emission was dominated by a hot gaseous isothermal halo (Forman, Jones, & Tucker 1985), was questioned because of discrepancy with the flat H I rotation curve (Knapp 1987).

This paper is mostly based on the analysis of high-resolution *ROSAT* HRI (see Trümper 1983 for a description of the satellite) X-ray images of the Sombrero galaxy. The purpose of our *ROSAT* HRI observations of this galaxy was to investigate more thoroughly its X-ray morphology and address some of the questions left unanswered by the *Einstein* data, by obtaining higher ( $\sim 5''$  FWHM) angular resolution data. These data allow us for the first time to investigate directly individual components of the X-ray emission, and in particular to study the nucleus in X-rays.

This galaxy was also observed with the other instrument on *ROSAT*, the PSPC (Ruiz, Forman, & Jones 1996). The PSPC has a wider point spread function (PSF) than the HRI ( $\sim 50''$  FWHM), and spectral capabilities ( $\Delta E/E \sim 1$ ). The PSPC data now being publicly accessible, we have also taken a look at them, to complement our work and seek spectral information.

### 2. OBSERVATIONS AND DATA ANALYSIS

The data were analyzed with the IRAF/xray package developed at SAO in collaboration with NOAO. Details are given below.

#### 2.1. HRI Observations

Table 1 summarizes some of the parameters of NGC 4594 and gives the log of the observations. The Sombrero galaxy

TABLE 1  
NGC 4594 PARAMETERS AND ROSAT HRI OBSERVATIONS

Type	R.A. Decl. (J2000)		$L_B^a$ ( $L_\odot$ )	$D^b$ (Mpc)	$N_H^c$ ( $\text{cm}^{-2}$ )	$L_X^d$ ( $\text{ergs s}^{-1}$ )	Observation Dates (start/stop)	Livetime (s)
Sa/Sb.....	12 39 59,	-11 37 23	$2.1 \times 10^{11}$	18	$3.5 \times 10^{20}$	$1.1 \times 10^{41}$	A. 1992 Jan 11 B. 1993 Dec 30/1994 Jan 7 C. 1994 Jul 09/1994 Jul 17	1632 3643 15688

<sup>a</sup> From the extinction corrected apparent magnitude of RSA.

<sup>b</sup> From RSA, with  $H_0 = 50$ .

<sup>c</sup> From Stark et al. 1992.

<sup>d</sup> (0.2–4.) keV *Einstein* luminosity from Fabbiano, Kim, & Trinchieri 1992. This luminosity has been scaled to the RSA distance. It was calculated for a hard 5 keV spectrum.

was observed for three distinct intervals with the ROSAT HRI (see David et al. 1995 for a description of the HRI characteristics), widely separated in time, for a total of 20,963 s. We label these intervals A, B, and C for future reference. The HRI has a spatial resolution FWHM  $\sim 5''$  and an instrumental pixel size of  $0''.5$ . Visual inspection of the processed data, including the standard aspect correction provided by the ROSAT Data Center, shows that while the first two segments (A and B) present a pattern of X-ray sources with consistent positions, the third, and longest segment (C) presents a similar pattern, but displaced in both coordinates. The displacement amounts to  $-4''.5$  in the east–west and  $-1''$  in the north–south direction, respectively. This effect is due to an erroneous calculation of the pointing direction of the satellite. To obtain a merged image of the entire HRI observation, we have applied a correction by “shifting back” in software the field positions of segment C to those of the first two segments. While the merged image gives an accurate picture of the distribution of X-ray sources in NGC 4594, the absolute positions are uncertain by at least the amount of the “shift” between data segments. However, the presence of a bright G0 star in the field

(see below) gives us a way to obtain more accurate positions for the X-ray sources.

2.2. Spatial Distribution of the X-Ray Surface Brightness

Figure 1a shows a gray-scale representation of the central part of the merged NGC 4594 field binned in  $1''$  pixels and smoothed with a  $4''$   $\sigma$  Gaussian. This figure shows a region of X-ray emission extending for  $\sim 2'$  along the plane of the galaxy, and some distinct clumps or pointlike sources. Of these, one (source 2) appears to coincide with a bright 9.7 mag G0 star (HD 110086). The other prominent source (No. 5) is in the nuclear region of NGC 4594. An overlay of this contour map on the optical image from the digitized STScI sky survey is shown in Figure 1b.

To quantify the spatial extent of the X-ray emission of NGC 4594, we derived a radial profile in  $5''$  radial bins of the entire (source plus background) detected HRI counts centered on the nuclear strong source. We omitted circular regions of  $10''$  radii centered on sources which appear unconnected with NGC 4594 (sources 1, 2, 8 of Table 2). This radial profile (Fig. 2a) shows that the field background is radially uniform for radii larger than  $180''$ . The back-

TABLE 2  
SOURCE FLUXES AND LUMINOSITIES

Source	Position <sup>a</sup> (pixels)		Radius	Counts	Count Rate ( $\text{counts s}^{-1}$ )	$F_X^b$ ( $\text{ergs s}^{-1} \text{cm}^{-2}$ )	$L_X$ ( $\text{ergs s}^{-1}$ )
	(J2000 R.A., Decl.)						
1 .....	5082	3724	15	$32.7 \pm 8.3$	$1.56 \times 10^{-3}$	1.01	
	12 39 26.38,	11 40 10.6	10	$20.0 \pm 6.5$	$9.53 \times 10^{-4}$	0.64	
2 .....	4528	3886	15	$92.6 \pm 11.7$	$4.42 \times 10^{-3}$	2.89	
	12 39 45.21,	-11 38 49.6	10	$72.0 \pm 10.0$	$3.43 \times 10^{-3}$	2.30	
3 <sup>c</sup> .....	4436	4076	10	$14.8 \pm 6.0$	$7.06 \times 10^{-4}$	0.47	$1.8 \times 10^{39}$
	12 39 48.34,	-11 37 14.6					
4 .....	4168	4068	10	$23.8 \pm 6.8$	$1.14 \times 10^{-3}$	0.76	$2.9 \times 10^{39}$
	12 39 57.45,	-11 37 18.6					
5 .....	4111	4060	15 <sup>d</sup>	$291.9 \pm 18.7$	$1.39 \times 10^{-2}$	9.04	$3.5 \times 10^{40}$
	12 39 59.39,	-11 37 22.6 <sup>e</sup>	10	$247.9 \pm 17.1$	$1.18 \times 10^{-2}$	7.90	$3.1 \times 10^{40}$
6 .....	4064	4061	10	$70.9 \pm 10.0$	$3.38 \times 10^{-3}$	2.26	$8.8 \times 10^{39}$
	12 40 0.98,	-11 37 22.1					
7 .....	4036	4074	10	$21.4 \pm 6.6$	$1.02 \times 10^{-3}$	0.68	$2.6 \times 10^{39}$
	12 40 1.93,	-11 37 15.6					
8 .....	3858	5197	15	$34.7 \pm 8.5$	$1.65 \times 10^{-3}$	1.07	
	12 40 7.99,	-11 27 54.1	10	$31.0 \pm 7.4$	$1.48 \times 10^{-3}$	0.99	

<sup>a</sup> One pixel is 0.5 arcsec. R.A., decl. are derived using the position of the G0 star HD 110086, associated with source 2.

<sup>b</sup> To derive (0.1–2.4 keV)  $F_X$ , we assumed an encircled energy of 0.85 and 0.875 for extraction radii of  $10''$  and  $15''$ , respectively.

<sup>c</sup> Below the  $3\sigma$  threshold.

<sup>d</sup> Excluding a  $10''$  circle centered on source 6.

<sup>e</sup> R.A. = 12 39 59.40, decl. =  $-11 37 23.0$  (J2000) for the radio nucleus (Bajaja et al. 1988).

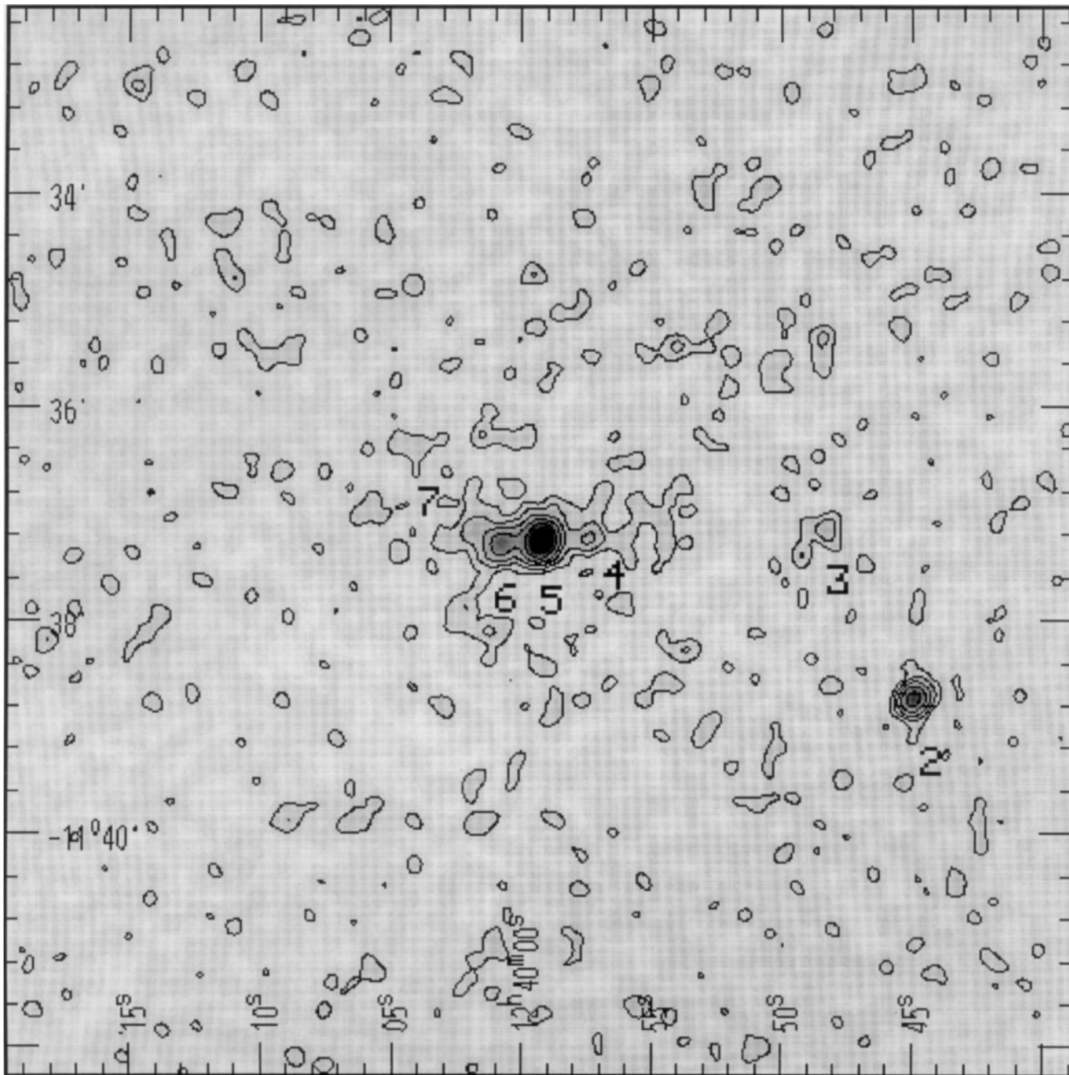


FIG. 1a

FIG. 1.—(a) X-ray gray-scale representation and contour map of the central portion of the merged NGC 4594 image. Data were binned in  $1''$  pixels (two instrument pixels), and smoothed with a Gaussian of  $\sigma = 4''$ . Contours are in logarithmic scale, the lowest is plotted at 4% of peak intensity, the highest is at 100% of peak intensity. The numbers identify the emission regions listed in Table 2. (b) Same contour map overlaid onto the STScI digitized sky survey place of NGC 4594. We have used the bright G0 star (source 2) to align the X-ray and optical maps. Notice the bright X-ray source at the nucleus.

ground subtracted profile is shown in Figure 2b. This was derived by using an annulus of 375–425 pixels radii ( $187''.5$ – $212''.5$ ) centered on the strong source at the center of the galaxy. Most of the radial extent is due to the east–west elongated emission region (see Fig. 1). To make sure that possible errors in the merging of the three data segments would not result in smearing of the innermost part of the radial profile, we repeated this procedure using the data from segment C only. No appreciable differences can be seen, within statistics.

Figure 2c shows again the background subtracted radial profile in the innermost region (*circles*), together with a north–south profile (*filled squares*) obtained by using azimuthal sectors of 90 degrees along the north–south axis. The north–south profile is clearly dominated by the central source. We do not find significant evidence of diffuse emission in this direction past  $25''$ . The north–south profile, however, is not consistent with a single point source, suggesting the presence of an extended emission component in

the bulge of NGC 4594. This can be seen by comparing the north–south profile with either a similarly binned PSF model (*stars*) or with a smeared PSF model that was derived to take into account possible aspect uncertainties (*crosses*). The latter was derived by adding together five PSF models, one at the center and the other four displaced by  $5''$  in a cross pattern. This is possibly a worst case depiction of such an effect.

With our data it is difficult to extract cleanly a nuclear point source. The problem is to estimate the effect of the galactic disk and inner bulge emission. While we do not have enough sensitivity to model this with our observations, we tried using the region of the disk to the west of the nucleus to estimate the disk background. This was done by using a region confined between  $\pm 45^\circ$ , from the east–west line and extending radially between  $20''$  and  $40''$  from the centroid of the central source. The resulting profile is also plotted in Figure 2c (*diamonds*), and it can be seen that it is consistent with an aspect-smearred point source. The radial

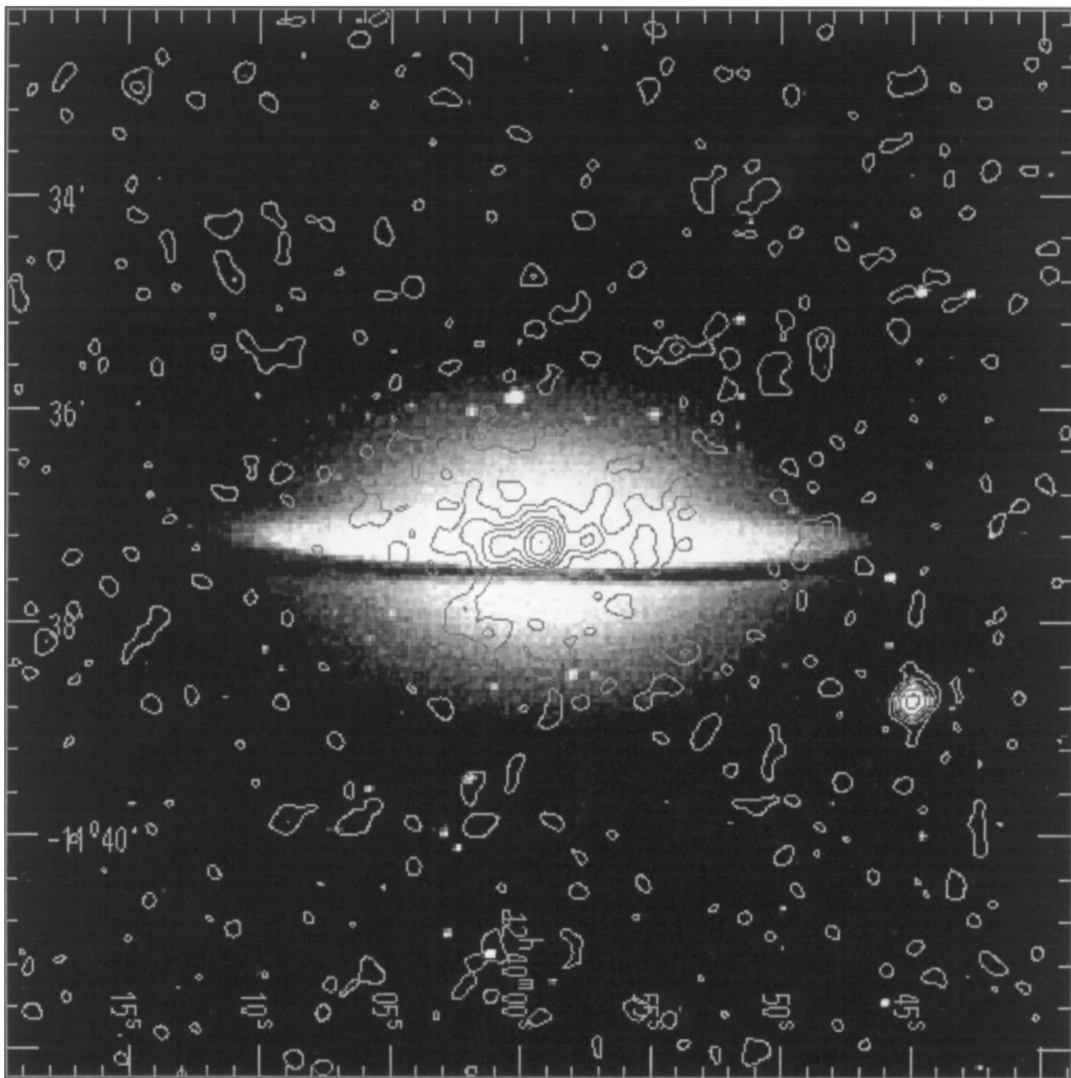


FIG. 1b

profile of source 2 (the G0 star) is also consistent with this distribution (*filled circles*), confirming that the nuclear source is pointlike.

### 2.3. Count Extraction and Fluxes

We estimated source counts following two different approaches: (1) we used the contour maps and radial profiles as a guide to select regions of the field for count extraction; (2) we ran the IRAF/xray “*ldetect*” program, for a range of count extraction cells going from 12 to 36 square arcsec. We then used the centroid of the “*ldetect*” sources as a guide for count extraction. We did not use the count and signal-to-noise estimates from “*ldetect*” directly because the sliding centroid method on which “*ldetect*” is based will give a faulty determination of the field background in crowded areas. To estimate the field background, we used the same background annulus described in § 2.2.

In Table 2 we list eight sources found by these methods. With the exception of source 3, they are all above the  $3\sigma$  detection threshold. We also list source 3 (at  $2.5\sigma$ ), to give a feel for the significance of the count excesses seen in Figure 1a. Of these sources, 4, 5, 6, and 7 are associated with the crowded area along the galaxy disk. Sources 5 and 6 are relatively strong. Source 5 appears associated with the

nuclear region. Sources 4 and 7 are at our detectability threshold and could just be local enhancement of the surface brightness. As remarked in § 2.2, source 2 coincides (within the aspect uncertainty) with a bright G0 star. We find that the X-ray to optical ratio for this source is  $f_X/f_V = 10^{-3.4}$ . This is consistent, although slightly higher, with the range  $f_X/f_V$  found by Vaiana et al. (1981) for G0 stars ( $10^{-6.5}$  to  $10^{-3.6}$ ), suggesting that the star is the X-ray source.

Centroids used for source and background extraction, and radii of the extraction circles are listed in Table 2, together with net counts with statistical error, count rates, (0.1–2.4) keV fluxes, and luminosities for the sources likely to be associated with NGC 4594 on the basis of positional coincidence. The source positions are given both in instrumental pixels and in J2000 R.A. and decl., based on the accurate optical position of source 2 (the G0 star HD 110086). The position of source 5 is consistent with that of the radio nucleus.

The count rates were derived from the detected counts by dividing by the total observing time. To estimate fluxes these rates were corrected by the appropriate encircled energy factor (see Table 2); the conversion from corrected rates to flux was then done using an assumed power-law spectrum with  $\alpha_E = 1.0$  and the  $N_H$  listed in Table 1. Given that these data do not permit a determination of the spec-

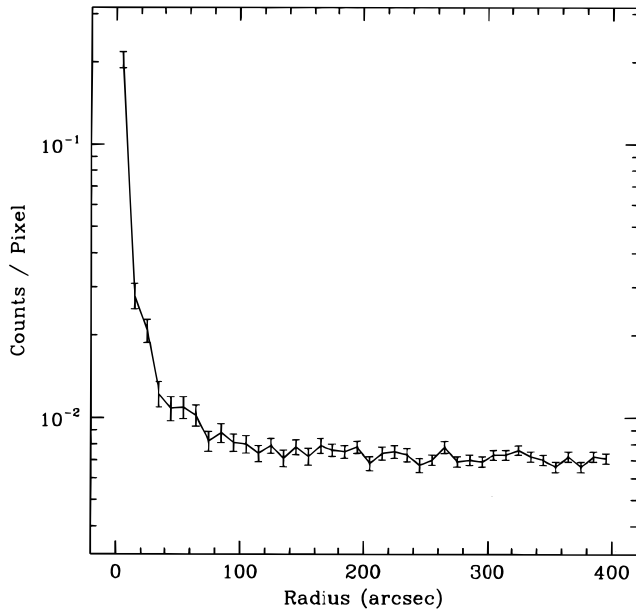


FIG. 2a

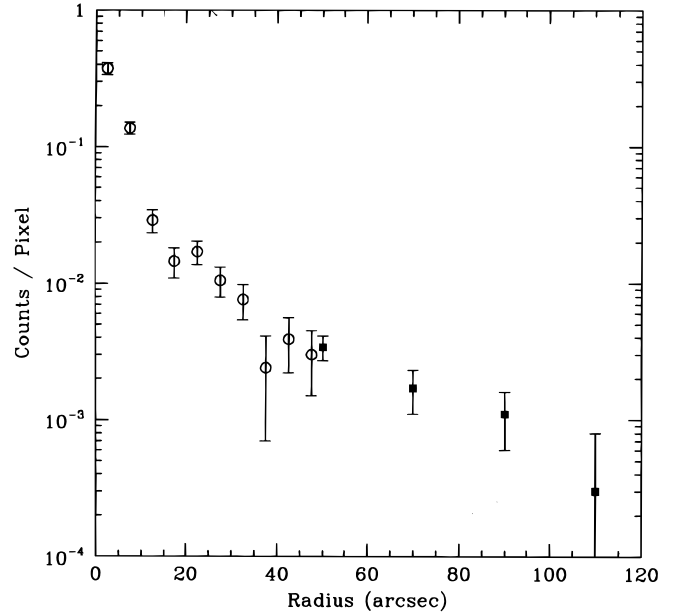


FIG. 2b

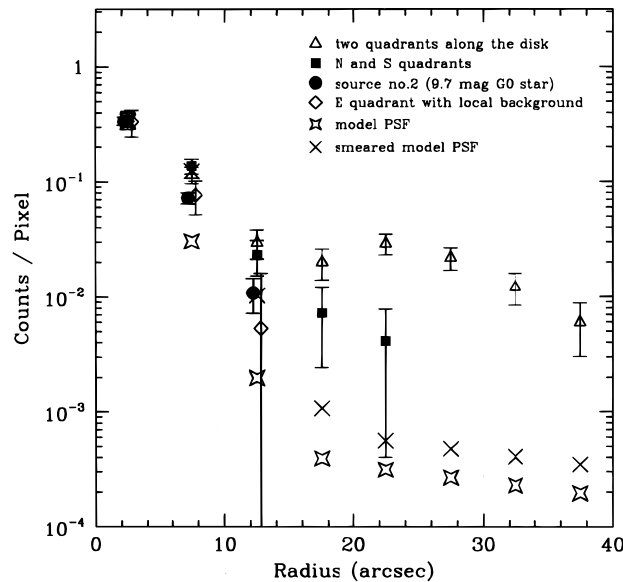


FIG. 2c

FIG. 2.—(a) Radial profile of the total (sources plus background) HRI counts centered on the nucleus of NGC 4594 (source 5). We have omitted circular regions of  $10''$  radii centered on sources 1, 2, and 8 (see Table 2), which appear unconnected with NGC 4594. (b) Background subtracted radial profile of NGC 4594. The background was derived from the annulus of radii  $187''.5$  and  $212''.5$ . (c) Background subtracted radial profile and PSF in the  $r \leq 40''$  region. Background derived as in (b) except than in the case of the quadrant toward east profile (diamonds), where the background was extracted locally from a region with  $20'' < 40''$ . The different profiles are described in the text.

tral parameters, we estimate an uncertainty on the fluxes of a factor of 2, for a range of power laws with  $\alpha_E$  from 0.5 to 2.0.

For the nuclear source (No. 5), we also estimated the net counts from a  $15''$  circle using a disk background estimate (see § 2.2). We obtain  $267.4 \pm 19.7$  net counts, which differs less than 10% from the value obtained using a field background.

Besides extracting counts from individual sources or clumps of emission, we also estimated the total emission from different galaxy components. The results are summarized in Table 3. Here we give first the total emission from a circular extraction regions of  $125''$  radius and the same background region used in Table 2. This is the extent

suggested by the radial profiles of Figure 2a. We also explored the possibility of low surface brightness emission at larger radii by using a larger extraction radius ( $250''$ ) and background from a  $300''$ – $350''$  annulus. We obtain more net counts but the increase is not statistically significant. The results are listed in Table 3. Use of this different background extraction area does not change appreciably the source counts of Table 2. In Table 3 we also give the results for a “disk” count extraction area ( $500''$  by  $40''$  box extending along the major axis of NGC 4594), the sum of the discrete source contribution within the “disk,” region.

A PSPC observation of the NGC 4594 field (Ruiz et al. 1996) shows a relatively bright source at J2000 12:40:03.5,  $-11:39.35$ , which is not present in our HRI data. We have

TABLE 3  
NGC 4594 GALAXY COMPONENTS: FLUXES AND LUMINOSITIES

	Regions (arcsec)	Counts	Count Rate (counts s <sup>-1</sup> )	$F_X^a$ ( $\times 10^{-13}$ ) (ergs s <sup>-1</sup> cm <sup>-2</sup> )	$L_X^a$ (10 <sup>40</sup> ergs s <sup>-1</sup> )
Total1 .....	circle: $r = 125$	$681 \pm 68$	$3.25 \times 10^{-2}$	18.5	7.2
Total2 .....	circle: $r = 250$	$846 \pm 135$	$4.04 \times 10^{-2}$	23.0	8.9
Disk .....	box: $500 \times 40$	$528 \pm 36$	$2.52 \times 10^{-2}$	14.3	5.6
Bulge .....	total 2 – disk	$318 \pm 140$	$1.52 \times 10^{-2}$	8.64	3.4
Point sources .....	no. 4, 5, 6, 7	$409 \pm 24$	$1.95 \times 10^{-2}$	11.1	4.3

<sup>a</sup> In the (0.1–2.4 keV) range.

derived a flux for this source using the archival PSPC data rp600258. Within a 90" radius circular region, we obtain  $329 \pm 22$  net source counts, corresponding to a (0.1–2.4 keV) flux of  $7.2 \times 10^{-13}$  ergs cm<sup>-2</sup> s<sup>-1</sup>. By comparison, using an HRI 15" extraction circle we obtain  $-0.43 \pm 5.6$  net counts, giving a 3  $\sigma$  upper limit of  $4.8 \times 10^{-14}$  ergs cm<sup>-2</sup> s<sup>-1</sup> on the X-ray flux.

#### 2.4. Variability

We searched for possible variability in the two strong detected sources in NGC 4594 (sources 5 and 6), by extracting count rates by the methods described above in different contiguous observing time intervals, ranging from 1.3 to 4 ks. The results are shown in Figure 3 and Table 4. While the count rates of source 6 are constant within statistics, there is a suggestion of possible variability in source 5, the nucleus of NGC 4594. We performed  $\chi^2$  tests to quantify how the observed count rates differ from a constant average emission. We find a  $\chi^2 = 15.8$  for 8 degrees of freedom in the case of the nuclear source (source 5), giving a probability of chance occurrence  $P \sim 4.5\%$ . In the case of source 6, we obtain  $\chi^2 = 6.2$  for 8 degrees of freedom, giving a probability of chance occurrence  $P \sim 62\%$ . This suggests that the nuclear source may be time variable. Future more sensitive observations will be needed to explore this point further.

#### 2.5. Spectral Properties of the Emission

The best existing X-ray spectra of NGC 4594 were obtained with ASCA (Terashima et al. 1994; Serlemitsos et al. 1996) and suggest the presence of a hard, intrinsically absorbed nuclear source plus some thermal emission. The ASCA data, however, do not have enough spatial resolution to derive unambiguously the properties of the various components of this complex X-ray source. We therefore tried to glean spectral information from the ROSAT data. The ROSAT HRI has very crude and poorly calibrated energy resolution (David et al. 1995), which can be used to investigate differences in hardness ratios between different com-

ponents of the image. With our data we did not find any significant trends, although there may be a suggestion of source 6 being softer than the nucleus. The hardness ratio of the nucleus is entirely consistent with that of the integrated emission of NGC 4594 (nucleus excluded). NGC 4594 was also observed with the ROSAT PSPC, resulting in a 10,575 s livetime (see Ruiz et al. 1996). These data (rp600258) are now in the ROSAT Archive, and we used them to derive the spectral parameters of the emission.

Details of the PSPC analysis are given in the Appendix. In summary, we find that even with the PSPC we cannot isolate the nuclear source to obtain its uncontaminated spectrum. Given the PSPC PSF, of the order 50% of the

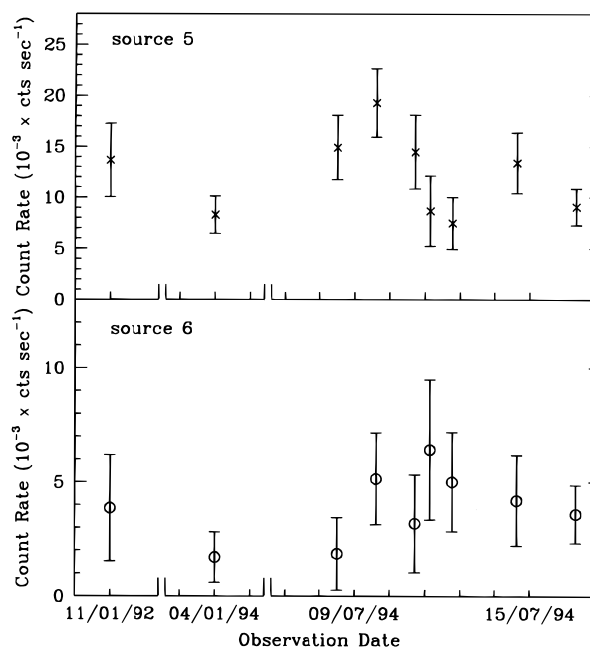


FIG. 3.—Light curves of sources 5 (the nucleus) and 6, derived from the data in Table 4.

TABLE 4  
TIME VARIABILITY

Interval	Time(begin) (date, time)	Time(end) (date, time)	Time(live) (s)	Counts <sup>a</sup> (err)	
				Source 5	Source 6
1 .....	1992 1 11, 12:36:42	1992 1 11, 13:05:03	1632	22.3(5.9)	6.3(3.8)
2 .....	1993 12 30, 13:43:51	1994 1 7, 15:55:57	3643	30.2(6.7)	6.2(4.0)
3 .....	1994 7 9, 03:21:53	1994 7 9, 04:02:10	2146	32.0(6.8)	4.0(3.4)
4 .....	1994 7 9, 04:47:58	1994 7 11, 16:06:15	2332	45.0(7.8)	12.0(4.7)
5 .....	1994 7 11, 16:06:16	1994 7 11, 17:48:04	1678	24.3(6.1)	5.3(3.6)
6 .....	1994 7 11, 17:48:05	1994 7 12, 15:59:07	1336	11.6(4.6)	8.6(4.1)
7 .....	1994 7 12, 15:59:08	1994 7 13, 04:39:19	2017	15.1(5.1)	10.1(4.4)
8 .....	1994 7 13, 04:39:20	1994 7 16, 23:18:58	2171	29.1(6.5)	9.1(4.3)
9 .....	1994 7 16, 23:18:55	1994 7 17, 01:21:09	4008	36.4(7.2)	14.1(5.1)

<sup>a</sup> Counts are from 10" radius circular regions centered on the sources 5 and 6.

counts from the central source will arise from the disk emission visible in our HRI image. Spectral fits of these data to power-law models result in a best-fit power law with  $\alpha_E \sim 0.8$ . However, the quality of the data does not allow us to distinguish between power-law and other spectral shapes. Two-component models with nuclear and non-nuclear components cannot be constrained usefully.

The count rate outside of the central nuclear source region is too low to constrain usefully the spectral parameters of the galaxy bulge emission. Between  $2'$  and  $6'$  galactocentric radii, we can set only a lower limit of  $kT > 0.8$  keV (90% confidence) for a fit with a Raymond-Smith thermal model with 20% solar abundance.

Fairly high values of  $kT$  ( $> 1.2$  keV) are also obtained fitting all of the detected PSPC source counts with thermal Raymond-Smith models. This result, however, is likely to reflect the presence of a hard nuclear source (see *ASCA* results).

### 3. DISCUSSION

#### 3.1. The X-Ray Emission of NGC 4594

Our HRI image of NGC 4594 has shown that the X-ray emission is complex, consisting of a bright nuclear source, a few sources or emission regions extending along the disk of the galaxy, and some diffuse (or not resolved) emission in the bulge.

We detect clearly emission from a 2.6 kpc radius region in the inner disk of NGC 4594 (Fig. 1). If this emission is due to a few discrete sources, each source (Table 2) has a luminosity well above that of the brightest X-ray sources in M31 (e.g., Trinchieri & Fabbiano 1991), and also above that of the sources detected with *Einstein* in M81, the brightest of which (M81 X-6) was detected with an  $L_X \sim 2 \times 10^{39}$  ergs  $s^{-1}$  (Fabbiano 1988). If these emission clumps are due to individual close accreting binaries, their exceptional luminosity would imply the presence of massive accreting black holes. An alternative explanation is that nonnuclear inner-bulge emission may be instead indicative of a rotationally flattened cooling flow in a hot ISM (W. Matthews, private communication; Brighenti & Matthews 1996). This is an intriguing possibility, which however cannot be pursued further with the present data.

Table 3 shows that there is an integrated “diffuse” (excluding detected point sources)  $L_X \sim 1.3 \times 10^{40}$  ergs  $s^{-1}$  from the disk region and an integrated diffuse  $L_X \sim 3.4 \times 10^{40}$  ergs  $s^{-1}$  from the bulge/halo region. If this diffuse emission is due to a hot extended gaseous component in hydrostatic equilibrium with the galaxy potential, the X-ray data may be used to measure the mass of the Sombrero galaxy. This was attempted by Ruiz et al. (1996) using the PSPC data. However, from the analysis of the PSPC data we cannot draw any conclusions on the nature of this diffuse emission, because the presence of the strong nuclear source makes these results uncertain in the central region, and the count statistics are too low at larger radii (see § 2.5 and the Appendix). The use of these data for measuring the binding mass of the Sombrero galaxy is premature at best, and such measurements are heavily model and assumption dependent. The *ASCA* data (Terashima et al. 1994) have been reported to show some extended emission line contribution, but a detailed quantitative analysis has not yet been published, and in any event they have limited spatial information.

With the HRI, we cannot establish how much of this emission is due to a truly diffuse gaseous component, and how much can be explained with the integrated contribution of sources below the detection threshold. The point source detection threshold of the HRI observation is  $\sim 2 \times 10^{39}$  ergs  $s^{-1}$ , well above the luminosity of most individual X-ray sources in Local Group galaxies and M81. Therefore such sources would not be detected individually, but they would contribute to the diffuse emission. To further explore this point, we compared the X-ray properties of NGC 4594 with those of the better understood nearby galaxies M31 and M81, which are both early-type spirals with prominent bulges. The results are summarized in Table 5. The optical luminosities ( $L_B$ ) were derived from two different catalogs, the RSA (Sandage & Tamman 1981), and Tully (1988). The M31 and M81  $L_B$  values from the RSA are larger than those from Tully (1988). In both cases, NGC 4594 (nucleus excluded) is relatively more luminous in X-rays than M31. If the RSA estimates are more accurate, this is also true for the comparison with M81. These results may suggest that NGC 4594 may have X-ray emission in excess of the purely X-ray binary component that dominates in M31, and therefore perhaps some hot ISM. However, M81 (nucleus excluded) is also overluminous in X-rays when compared to M31, but its *Einstein* luminosity used in Table 5 (Fabbiano 1988) is dominated by individual bright sources. Therefore, based on the presently available data, we cannot draw any strong conclusion on the amount and distribution of a hot ISM in the Sombrero galaxy. We will have to wait for sensitive, spatially and spectrally resolved AXAF data.

#### 3.2. The LINER Nucleus

NGC 4594 has a LINER nucleus (Heckman 1980; L. Ho 1995, private communication), which also hosts a compact and variable radio continuum source (e.g., Hummel et al. 1984; Bajaja et al. 1988). There is dynamical evidence pointing to a massive ( $\sim 5 \times 10^8 M_\odot$ ) concentration, possibly a black hole at this nucleus (see Kormendy & Richstone 1995, and references therein).

We have discovered a pointlike X-ray source at this nucleus, with a (0.1–2.4 keV) luminosity of  $\sim 3 \times 10^{40}$  ergs  $s^{-1}$ . The characteristics of this source point to a low-luminosity AGN. The X-ray luminosity is significantly in excess of that detected from “typical” single accretion binaries in nearby galaxies. Similarly, in a projected physical volume corresponding to that of the central source count extraction region, the integrated luminosity of many tens of relatively bright pointlike X-ray binaries in M31 is  $\sim 1\text{--}2 \times 10^{39}$  ergs  $s^{-1}$ , only  $\sim 5\%$  of that of the nucleus of NGC 4594. The suggestion of variability (§ 2.4), if confirmed, would support the presence of a single compact X-ray source at the nucleus.

From the point of view of optical line emission, the X-ray nucleus of NGC 4594 compares well with other low-luminosity AGN. Its total  $H\alpha$  luminosity (L. Ho 1995, private communication) is  $4 \times 10^{39}$  ergs  $s^{-1}$  for the distance adopted in this paper ( $D = 18$  Mpc). The  $H\alpha$  and X-ray luminosities are in the range of those found in five low-luminosity AGN (LLAGN) studied with *ROSAT* and also of the nucleus of M81 (see Koratkar et al. 1995). The X-ray luminosity of the NGC 4594 nucleus is also consistent with that expected given its radio continuum luminosity, on the basis of the X-ray radio continuum

TABLE 5  
COMPARISON OF NGC 4594 WITH M31 AND M81

Galaxy (1)	$D$ (Mpc) (2)	$\log [L_X(\text{nonnuclear})]$ ( $\text{ergs s}^{-1}$ ) (3)	$\log (L_B)^a$ ( $L_\odot$ ) (4)	$\log (L_X/L_B)$ ( $\text{ergs s}^{-1}/L_\odot$ ) (5)
NGC 4594.....	18	40.78	11.29 <sup>b</sup> 11.32 <sup>c</sup>	29.49 29.46
M31.....	0.7	39.48 <sup>d</sup>	10.46 <sup>b</sup> 10.83 <sup>c</sup>	29.02 28.65
M81.....	3.6	39.98 <sup>e</sup>	10.33 <sup>b</sup> 10.81 <sup>c</sup>	29.65 29.17

<sup>a</sup>  $L_B = \text{dex} [0.4(5.48 - M_B)]$ , where  $M_B$  is the absolute magnitude derived from the total blue apparent magnitude corrected for reddening.

<sup>b</sup> Using absolute magnitudes from Tully 1988, corrected for the distance in col. (2).

<sup>c</sup> Using absolute magnitudes from the RSA, corrected for the distance in col. (2).

<sup>d</sup> From Trinchieri & Fabbiano 1991.

<sup>e</sup> From Fabbiano 1988.

correlation of bright radio galaxies (Fabbiano et al. 1984). In this regard, the NGC 4594 nucleus behaves like a down-sized version of a bright AGN. Moreover, we find that the optical to X-ray spectral index ( $\alpha_{\text{ox}}$ ) of this nucleus is consistent with the  $\alpha_{\text{ox}} - X$ -ray luminosity trend found for both radio-loud and radio-quiet quasars, i.e., fainter objects tend to be relatively more X-ray bright (Worrall et al. 1987: see Bechtold et al. 1994), although the dispersion about the best fit relation is very large. For the nucleus of NGC 4594 we derive  $\alpha_{\text{ox}} = 0.9$  (see also Fabbiano 1996), within the expected range for the X-ray luminosity of this nucleus ( $\alpha_{\text{ox}} = 0.6$  for radio-loud and  $\alpha_{\text{ox}} = 1.0$  for radio-quiet quasars).

Figure 4 compares the global spectral energy distribution (SED) of the nucleus of NGC 4594 with that of other three low-luminosity AGN/LINERs (the nucleus of M81 in high state, from the compilation of Ho, Filippenko, & Sargent

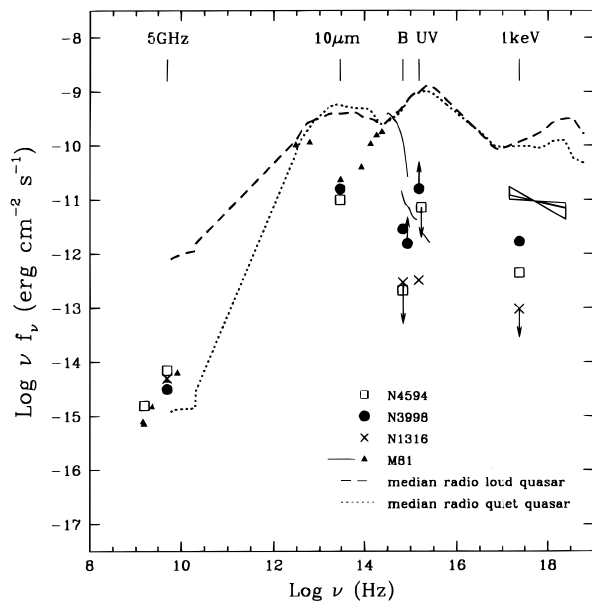


FIG. 4.—A comparison of the spectral energy distribution (SED) of the nucleus of NGC 4594 to the nuclei of NGC 1316, NGC 3998, M81, and the median of radio-loud and radio-quiet quasars. For the nucleus of NGC 4594, radio data are from Hummel et al. 1984 and Bajaja et al. 1988, the IR point is from Willner et al. 1985, the optical is from Crane et al. 1993, and the UV point is from Kinney et al. 1993. Data of NGC 3998 and NGC 1316 nuclei are from Fabbiano, Fasnacht, & Trinchieri 1994. The electronic version of M81 data are from L. Ho (private communication), and the data of radio-loud and radio-quiet quasar are from Elvis et al. (1994).

1996; the nuclei of NGC 3998 and NGC 1316, from Fabbiano, Fasnacht, & Trinchieri 1994; Fabbiano et al. 1992; Kim, Fabbiano, & Mackie 1996) and two representative luminous AGN SEDs (radio-quiet and radio-loud, from Elvis et al. 1994). The SEDs of NGC 1316 and NGC 3998 are not corrected for reddening in the optical-UV range (Fabbiano et al. 1994). However, the extraordinary blueness of the spectra argues for reddening to be unimportant. The M81 SED is reddening corrected, but this correction may still be underestimated (Ho et al. 1996). The optical point for NGC 4594 is from Crane et al. (1993), and no correction for intrinsic reddening has been applied. The UV point was derived from the *IUE* spectrum of Kinney et al. (1993) and, as remarked by these authors, is dominated by stellar emission. For this reason we plot it as an upper limit.

Ho et al. (1996), based on the SED of the nucleus of M81, suggested that LINER nuclei may be X-ray bright when their UV and X-ray emissions are compared to those of bright AGN. Our figure suggests a more confusing picture, with a marked lack of uniformity. The SEDs of the LINERs may be similar from the radio to the mid-IR (however, galactic contamination is likely at  $10 \mu\text{m}$ ), but then things change. In the  $B$ -UV range, in particular, the SEDs of the nuclei of NGC 3998 and NGC 1316, which are UV-bright (Fabbiano et al. 1994), follow the opposite trend to that of the nucleus of M81 (Ho et al. 1996). This variety of spectral shapes is not observed in bright AGN and QSO, whose spectra on the average are well represented by our template objects (Elvis et al. 1994). Relative to the radio emission, there is quite a dispersion of X-ray fluxes. There is also quite a dispersion of UV/X-ray ratios, from the X-ray bright M81 to the UV-bright NGC 3998. The NGC 4594 nucleus, in particular, is relatively radio-loud and its radio/X-ray ratio is comparable with that of radio-loud quasars.

If there is indeed a  $5 \times 10^8 M_\odot$  black hole at the nucleus of NGC 4594 (Kormendy & Richstone 1995) and the emission is powered by accretion onto this black hole (e.g., Rees 1984), our measure of the X-ray luminosity implies that we are in a highly sub-Eddington regime,  $L_X \sim 4 \times 10^{-7} L_{\text{Edd}}$ . This is also true if we use the total (2–10 keV) *ASCA* luminosity (Serlemitsos et al. 1996) of the hard (possibly nuclear) spectral component of NGC 4594 ( $L_X \sim 10^{-6} L_{\text{Edd}}$ ). In turn, this would imply very low accretion rates, and make NGC 4594 a candidate for a “low-state accretion disk” (Siemiginowska, Czerny, & Kostyunin 1996). If the Siemiginowska et al. model applies, the optical to UV spec-

tral energy distribution of the NGC 4594 nucleus should be rather flat, or even lacking UV. High spatial resolution observations of the nuclear region in the UV are needed to settle this point.

The SED of NGC 4594 does not seem to agree with the accreting black hole models that could explain the spectral energy distributions of the nucleus of M31 (also a LINER; Heckman 1996) and the Galactic center (Melia 1992, 1994). Even arguing that the IR may be contaminated by galactic dust emission, normalizing these models to the X-rays results in discrepancies in both the radio (overluminous relative to the models) and the optical (underluminous). These models, however, were calculated for black hole masses ranging from  $5 \times 10^6$  to  $10^7 M_\odot$  and accretion rates of  $\sim 10^{22}$ – $10^{24} \text{ g s}^{-1}$ . The accretion rate in the case of NGC 4594 could be substantially less, as discussed above. If we assume a typical accreted rest energy to luminosity conversion of 0.1 for a NGC 4594 nuclear black hole, the accretion rate at the present luminosity would be  $\sim 10^{20} \text{ g s}^{-1}$ . Moreover, the optical emission could be somewhat affected by presently unknown reddening.

It is also possible, however, that the nuclear source is significantly absorbed, and that the detected X-ray emission is not the direct emission from the nucleus, but perhaps reprocessed fluorescent photons form a surrounding obscuring disk or torus (e.g., as in NGC 1068; Ueno et al. 1994). The *ASCA* data suggest an absorbed hard nuclear component (Serlemitsos et al. 1996). This scenario may also be supported by the recent results on the polarization of the optical emission of NGC 4258 (Wilkes et al. 1996), an edge-on early-type spiral hosting a  $1.4 \times 10^7 M_\odot$  black hole at its nucleus (Miyoshi et al. 1995), which has  $L_X \sim 4 \times 10^{40} \text{ ergs s}^{-1}$  and is heavily absorbed (Makishima et al. 1994). Although there is no evidence from the *ROSAT* data of NGC 4594 of substantial excess  $N_H$  in the nucleus (§ 2.5), the signature of absorption may not be visible in the *ROSAT* range if the emission in this range is due to reprocessed radiation.

#### 4. SUMMARY AND CONCLUSIONS

The X-ray emission of NGC 4594, the Sombrero galaxy, has been decomposed into at least three components with the *ROSAT* HRI.

1. A pointlike, possibly variable nuclear source, responsible for one-third of the total emission with (0.1–2.4 keV)  $L_X \sim 3.5 \times 10^{40} \text{ ergs s}^{-1}$ . If this emission is due to accretion onto the  $5 \times 10^8 M_\odot$  black hole possibly present at the nucleus (Kormendy & Richstone 1995), the accretion rates must be very low, since the luminosity is extremely sub-Eddington. Alternatively, if obscuration is substantial, the detected nuclear flux may be due to reprocessed fluorescent photons and the intrinsic nuclear emission may be substantially higher.

2. Clumpy nonnuclear emission associated with the galaxy disk, with total  $L_X \sim 2.1 \times 10^{40} \text{ ergs s}^{-1}$ , most of which can be accounted for with three very luminous point like sources or clumps of emission. Each of these sources has an X-ray luminosity well above the Eddington luminosity for a  $1 M_\odot$  accreting compact object, suggesting that if the sources are X-ray binaries we are in the presence of relatively massive black holes. Lacking spectral information, however, or any evidence of variability, the above suggestion is purely speculative, and other explanations for the origin of this clumpy emission may be possible.

3. A bulge component with  $L_X \sim 3.4 \times 10^{40} \text{ ergs s}^{-1}$ . The latter is not resolved into individual sources, but the point-source threshold is high ( $L_X \sim 2 \times 10^{39} \text{ ergs s}^{-1}$ ), above the luminosity of X-ray sources detected in the bulge of M31. While comparison with M31 may suggest that this emission is largely due to a hot ISM, comparison with the nonnuclear emission of M81 leads to the opposite conclusion, that very little—if any—hot ISM may be present. A reanalysis of the PSPC data to obtain spectral constraints on the nature of the bulge emission has proved inconclusive, because of the insufficient spatial resolution of this instrument, combined with insufficient statistics.

With the present data the question of the amount and properties of a hot ISM in the Sombrero galaxy is still open, and therefore it is premature to attempt mass measurements for this galaxy based on hydrostatic equilibrium of a hot halo. However, we now know that the X-ray emission is complex and we have a clear measurement of the X-ray emission of the LINER nucleus.

We thank Martin Elvis, Aneta Siemiginowska, and Smita Mathur for useful discussions, Luis Ho for sharing with us some of his results before publication, Andy Ptak and Bill Mathews for comments on the preprint. This work was supported by NASA grant NAG5-1937 (*ROSAT*), NAGW 2681 (*LISA*), and NASA contract NAS8-39073 (*AXAF* Science Center). This research has made use of the following: NASA's Astrophysics Data System Abstract Service; Digitized Sky Survey, based on photographic data obtained using the UK Schmidt Telescope. The UK Schmidt Telescope was operated by the Royal Observatory Edinburgh, with funding from the UK Science and Engineering Research Council, until 1988 June, and thereafter by the Anglo-Australian Observatory. Original plate material is copyright the Royal Observatory Edinburgh and the Anglo-Australian Observatory. The plates were processed into the present compressed digital form with their permission. The digitized Sky Survey was produced at the Space Telescope Science Institute under US government grant NAG W-2166; NASA/IPAC Extragalactic Database; and SIMBAD, which is operated by the Centre de Données Astronomiques de Strasbourg (CDS), France.

## APPENDIX

### PSPC SPECTRAL ANALYSIS

#### 1. THE NUCLEAR SOURCE

Given the PSF of the PSPC (Hasinger et al. 1992) and the complexity of the X-ray emission in the central parts of NGC 4594 shown by our HRI data, it is impossible to isolate completely the nuclear source from the rest of the galaxy emission for the purpose of spectral analysis. An extraction radius of  $2'$  can be adequate for retaining most of the spectral counts from a

TABLE 6  
SUMMARY OF SPECTRAL RESULTS

$R^a$ (arcsec)	$R_1 - R_2^b$ (arcsec)	Range (keV)	Net Counts	$\log N_H^c$ ( $\text{cm}^{-2}$ )	$\alpha_E^c$	$kT$ (keV)	$\chi^2$	$\nu$
60.....	300–450	0.17–0.28 and 0.32–2.02	$895.5 \pm 35.6$	$20.72^{+0.18}_{-0.10}$	$0.76^{+0.44}_{-0.36}$	...	10.7	22
120.....	300–450	0.14–2.02	$1150.1 \pm 42.5$	$20.72^{+0.16}_{-0.12}$	$0.84^{+0.41}_{-0.29}$	...	13.1	24
120.....	190–300 <sup>d</sup>	0.14–2.02	$1131.9 \pm 42.1$	$20.73^{+0.14}_{-0.10}$	$0.84^{+0.36}_{-0.24}$	...	12.6	24
360.....	370–600 <sup>e</sup>	0.24–2.02	$1382.0 \pm 56.4$	$20.64^{+0.21}_{-0.19}$	...	2.2(>1.2)	19.6	21

<sup>a</sup> Radius of source extraction circle centered at the centroid of the nuclear emission, corresponding to PSPC pixels 7712, 7640.

<sup>b</sup> Radii of background extraction annuli. These have same center as source extraction circles.

<sup>c</sup> Uncertainties are at the 90% confidence for two interesting parameters.

<sup>d</sup> A circle centered at pixels 8150, 7450, with a radius of 50" was excluded from the background region. A bright source is found in this position.

<sup>e</sup> Circles centered at pixels 8150, 7450 and pixels 7580, 7380, with 60" radii were excluded from the source region. Bright sources not related with NGC 4594 are found in these positions.

point source, except in the case of very soft emission, where an extraction radius of 3' is recommended (M. Elvis 1995, private communication). Using an extraction radius of 1', 15%–20% of the photons near 0.1 keV would be lost, because of the wider PSF at the lower energies (Hasinger et al. 1992). With smaller extraction radii, the results would be even more severely biased. Our HRI image shows that a 1' radius circle centered on the nuclear source includes virtually all of the prominent "disk" emission. In this region we detect  $542 \pm 31$  net HRI counts, therefore the nucleus (Table 2) accounts for  $\sim 55\%$  of the emission. It accounts for  $\sim 43\%$  of the HRI counts from a 2' circle (see Table 3).

With the above in mind, we have extracted counts from 1' and 2' circles centered on the nucleus, with background from an annulus with the same center and 5'–7.5 radii. We have also subtracted a more "local" background from the 2' circle data, to see if inclusion of some of the low surface brightness emission would affect the results appreciably. This second background is from 3.2 to 5' radii, to exclude any possible spillover from the nuclear source. We have then fitted the data to power laws and thermal models. This analysis was done using the IRAF/xray/xspectral package. Details of the data extraction and a summary of the results for the power-law fits are given in Table 6. This shows that the 2' data are well fitted with a  $\alpha_E = 0.8$  power law with  $N_H = 5.3 \times 10^{20} \text{ cm}^{-2}$ , slightly above the line-of-sight value (Table 1). The alternative choice of background does not affect these results. Using a 1' circle for source extraction, the best-fit power law becomes flatter, consistent with softer photons being spilled out of the extraction circle. However, within the uncertainties the 1' and 2' parameters agree.

The data are equally well fitted with an exponential plus gaunt model and with a Raymond model with relatively low metal abundances (20% solar). A solar abundance Raymond model gives a significantly worse fit. In all cases, best-fit  $N_H$  values are consistent with the power-law results and best-fit  $kT$  are  $\sim 2$  keV or larger.

ROSAT spectra of Seyfert galaxies and low-luminosity active galaxies suggest steeper spectra for the nuclear source, with  $\alpha_E \sim 1.2$ –1.8 (Koratkar et al. 1995). We have attempted to fit the 2' PSPC data with a composite model, consisting of a nuclear source with some intrinsic absorption, with  $\alpha_E \sim 1.2$ –1.8, and accounting for between one- and two-thirds of the total 1 keV emission (reasonably consistent with the HRI results); and a second, thermal component, with line of sight absorption only. We find that the model parameters cannot be constrained.

## 2. THE BULGE ( $R > 2'$ )

Since the data within a 2' circle are mostly representative of the central emission, we attempted to fit the data from 2' to 6' to derive spectral parameters for the bulge diffuse emission reported by Ruiz et al. With a background from a 740"–1200" annulus, we obtain  $254 \pm 30$  net counts (0.17–1.9 keV). Fitting these data with a Raymond-Smith model with 20% solar abundances yields a fairly unconstrained  $kT > 0.8$  keV (90% confidence). We note that most of this emission originates from within 3' of the nucleus. We do not have a significant detection in the 3'–4' and 4'–6' annuli separately.

## 3. THE TOTAL EMISSION

Although we know that the emission is complex, it is worthwhile to extract and analyze the overall spectrum of NGC 4594, so that we can compare it with similar overall spectra of more distant galaxies for which spatial information is not available. To this end, we extracted the "total" PSPC galaxy emission within a 6' radius (see Table 6) and fitted it to Raymond-Smith models with solar and 20% solar abundances. The minimum  $\chi^2$  (for 21 degrees of freedom) decreases from 27.0 to 19.5 going from the solar to the 20% solar model. We list in Table 6 the results for the 20% solar case. The results are consistent with those of the fit of the 2' circle data with the same model.

## REFERENCES

- Bajaja, E., Dettmar, R.-J., Hummel, E., & Wielebinski, R. 1988, *A&A*, 202, 35  
 Bechtold, J., et al. 1994, *AJ*, 108, 759  
 Brighenti, F., & Matthews, W. G. 1996, *ApJ*, 470, 747  
 Crane, P., et al. 1993, *AJ*, 106, 1371  
 David, L. P., Harnden, F. R., Jr., Kearns, K. E., & Zombeck, M. V. 1995, US ROSAT Science Data Center/SAO report  
 Elvis, M. 1995, private communication  
 Elvis, M., et al. 1994, *ApJS*, 95, 1  
 Fabbiano, G. 1988, *ApJ*, 325, 544  
 ———. 1989, *ARA&A*, 27, 87  
 ———. 1996, in *ASP Conf. Ser.* 103, ed. M. Eracleous, A. Koratkar, C. Leitherer, & L. Ho (San Francisco: ASP), 56  
 Fabbiano, G., Fasnacht, C., & Trinchieri, G. 1994, *ApJ*, 434, 67

- Fabbiano, G., Kim, D.-W., & Trinchieri, G. 1992, *ApJS*, 80, 531
- Fabbiano, G., Miller, L., Trinchieri, G., Longair, M., & Elvis, M. 1984, *ApJ*, 277, 115
- Fabbiano, G., & Schweizer, F. 1995, *ApJ*, 447, 572
- Forman, W., Jones, C., & Tucker, W. 1985, *ApJ*, 293, 102
- Giacconi, R., et al. 1979, *ApJ*, 230, 540
- Halpern, J. P., & Steiner, J. E. 1983, *ApJ*, 269, L37
- Hasinger, G., Turner, T. J., George, I. M., & Boese, G. 1992, *GSFC OGIP Calibration Memo CAL/ROS/92-00*
- Heckman, T. M. 1980, *A&A*, 87, 152
- Heckman, T. 1996, in *The Physics of LINERs in View of Recent Observations*, ed. M. Eracleous & A. Koratkar (San Francisco: ASP), in press
- Ho, L. 1995, private communication
- Ho, L. C., Filippenko, A. V., & Sargent, W. 1996, preprint
- Hummel, E., van der Hulst, J. M., & Dickey, J. M. 1984, *A&A*, 134, 207
- Kim, D.-W., Fabbiano, G., & Trinchieri, G. 1992a, *ApJS*, 80, 645
- . 1992b, *ApJ*, 393, 134
- Kim, D.-W., Fabbiano, G., & Mackie, G. 1996, in preparation
- Kim, D.-W., Fabbiano, G., Matsumoto, H., Koyama, K., & Trinchieri, G. 1995, *ApJ*, 468, 175
- Kinney, A. L., Bohlin, R. C., Calzetti, P., Panagia, N., & Wyse, R. F. G. 1993, *ApJS*, 86, 5
- Knapp, G. R. 1987, in *Structure and Dynamics of Elliptical Galaxies*, ed. T. de Zeeuw (Dordrecht: Reidel), 145
- Koratkar, A., Deustua, S. E., Heckman, T., Filippenko, A. V., Ho, L. C., & Rao, M. 1995, *ApJ*, 440, 132
- Kormendy, J. 1988, *ApJ*, 335, 40
- Kormendy, J., & Richstone, D. 1995, *ARA&A*, 33, 581
- Makishima, K., et al. 1994, *PASP*, 46, L77
- Melia, F. 1992, *ApJ*, 398, L95
- Melia, F. 1994, *ApJ*, 426, 577
- Miyoshi, M., Moran, J., Herrnstein, J., Greenhill, L., Nakai, N., Diamond, P., & Inoue, M. 1995, *Nature*, 373, L127
- Pellegrini, S., & Fabbiano, G. 1994, *ApJ*, 429, 105
- Rees, M. J. 1984, *ARA&A*, 22, 471
- Ruiz, S., Forman, W., & Jones, C. 1996, *ApJ*, submitted
- Sandage, A., & Tammann, G. A. 1981, *A Revised Shapley-Ames Catalog of Bright Galaxies* (Carnegie Inst. of Washington Pub. 635), [RSA]
- Serlemitsos, P., Ptak, A., & Yaqoob, T. 1996, in *ASP Conf. Ser. 103*, ed. M. Evacleous, A. Koratkar, C. Leitherer, & L. Ho (San Francisco: ASP), 56
- Siemiginowska, A., Czerny, B., & Kostyunin, V. 1996, *ApJ*, in press
- Terashima, Y., Serlemitsos, P. J., Kunieda, H., & Iwasawa, K. 1994, in *New Horizon of X-Ray Astronomy—First Results from ASCA*, ed. F. Makino & T. Ohashi (Tokyo: Universal Academy Press), 523
- Trinchieri, G., & Fabbiano, G. 1991, *ApJ*, 382, 82
- Trinchieri, G., Kim, D.-W., Fabbiano, G., & Canizares, C. R. 1994, *ApJ*, 428, 555
- Trümper, J. 1983, *Adv. Space Res.*, 2, No. 4, 241
- Tully, R. B. 1988, *Nearby Galaxies Catalog* (Cambridge: Cambridge Univ. Press)
- Ueno, S., Mushotszky, R., Koyama, K., Iwasawa, K., Awaki, H., & Hayashi, I. 1994, *PASJ*, 46, L71
- Vaiana, G. S., et al. 1981, *ApJ*, 245, 163
- Wilkes, B. J., Schmidt, G. D., Smith, P. S., Mathur, S., & McLeod, K. 1996, *ApJ*, 455, L13
- Willner, S. P., Elvis, M., Fabbiano, G., Lawrence, A., & Ward, M. J. 1985, *ApJ*, 299, 443
- Worrall, D. M., Giommi, P., Tananbaum, H., & Zamorani, G. 1987, *ApJ*, 313, 596